Elastohydrodynamic films under periodic load variation. An experimental and theoretical approach

Romeo Glovnea, Xingnan Zhang
Department of Engineering and Design, University of Sussex, Brighton BN1 9QT, UK
Keywords: elastohydrodynamic, film thickness, vibrations, harmonic force

1. Abstract

The elastohydrodynamic lubrication regime occurs in systems where large elastic deformations, the hydrodynamic action of a converging wedge and eventually large variation of viscosity of the fluid concur to determine the formation of a continuous fluid film that separates the solid surfaces. Experimental and theoretical work, over the past few decades, have elucidated the role of various working and material parameters on the lubricant film thickness which plays a crucial role in protecting the solid surfaces from direct contact and ultimately from failure. These mechanisms are well understood for steady state conditions however, elastohydrodynamic contacts most often experience transient conditions, including variation of geometry, velocity of surfaces or load. In this case the mechanisms of film formation are more complex involving film squeeze in addition to the mechanisms mentioned above. Experimental and theoretical modelling of transient phenomena in elastohydrodynamic lubrication include sudden variation of entrainment speed or load and changing geometry. No systematic experimental study on the effect of harmonic load vibration upon the elastohydrodynamic films has been published before. In order to cover this gap this paper presents the results of an experimental study and of a simple theoretical approach on the behaviour of the elastohydrodynamic film thickness under harmonic variation of load.

2. Introduction

The formation of elastohydrodynamic (EHD) films, in steady-state conditions, is governed by the hydrodynamic action of the lubricant forced into a converging conjunction, the elastic flattening of the contacting surfaces and the variation of lubricant's viscosity with pressure. A theoretical, semi-analytical study, applied to linear contacts, by Ertel and Grubin [1, 2] and published by Grubin and Vinogradova, showed how these mechanisms contribute together to result in a parallel lubricant film separating the solid surfaces. The equation for the film thickness derived by Ertel/Grubin not only that revealed the physics of the phenomena but proved to be very close to more precise, later numerically derived formulas.

This important feature of a parallel lubricant film, over most part of the central region of the contact, was proved by many experimental results starting with those published by Gohar and Cameron [3, 4] who used optical interferometry to observe the film shape and measure the film thickness in circular, point contacts. The principles of optical interferometry, as applied to the study of EHD lubrication will be explained in a later section. An example of an image of a point contact is shown in Figure 1 captured by optical interferometry for PAO 40 (poly–alpha–olefin) oil, at an entrainment speed of 0.126 m/s, under 20 N normal contact load and at ambient temperature.

As seen, for most part of the central region of the contact the colour is uniform indicating a constant film thickness. This is because over that region the pressure is very large and varies little making the lubricant film almost unchanged until it reaches the outlet area of the contact, where a constriction in the film thickness occurs. The constriction, which also occurs at the sides of the contact, is a result of the rapid decrease of the pressure at the outskirts of the contact which must be accompanied by a change in film thickness in order to satisfy the pressure gradient condition imposed by Reynolds equation [2]. This feature is not included

in Ertel–Grubin analysis, although they were aware of the phenomenon and discussed it. Later, Greenwood [5] derived the exit constriction theoretically by moving the parallel region of the film off centre.

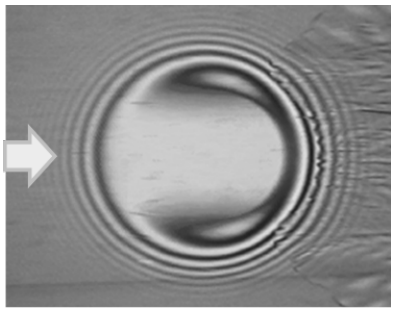

Figure 1. Example of contact image by optical interferometry

Early theoretical approaches of the lubricant film thickness in EHD contacts also include the works of Archard and Kirk [6] and Cameron and Gohar [7] focused on point rather than line contacts, however the real breakthrough in obtaining a reasonably accurate lubricant film thickness formula is due to Dowson and Higginson [8]. They solved numerically the coupled equations of the pressure in front of the contact (Reynolds), the film shape in that region (Hertz) and the variation of the lubricant's viscosity with pressure (Barus) to obtain an equation for film thickness for line contacts supported well by later experimental results. Later on, Dowson and co-workers [9, 10] have used the same method to solve the elliptical contact film thickness problem. A widely used relationship of the central film thickness in elliptical contacts is due to Hamrock and Dowson [9] and seen in Equation (1).

$$\frac{h_c}{R_x}=2.69\,\overline{U}^{0.67}\overline{G}^{0.53}\overline{W}^{-0.067}\left(1-0.61e^{-0.73\left(R_y/R_x\right)^{0.64}}\right) \qquad (1)$$

In this equation $\overline{U}$, $\overline{G}$ and $\overline{W}$ are respectively the speed, material and load non-dimensional parameters given by:

$$\overline{U}=\frac{U\eta_0}{E^*R_x},\ \overline{G}=\alpha E^*,\ \overline{W}=\frac{W}{E^*R_x^2} \qquad (2)$$

(U – entrainment speed, that is average speed of the surfaces in the direction of rolling, x, η_0, α – viscosity and pressure-viscosity coefficient of the lubricant at ambient pressure, W – load, E* – reduced elastic modulus of the solids, and R_x, R_y the reduced radii of curvature in the direction of entrainment and perpendicular to it, respectively). Equation (1) shows that the parameters with the strongest influence upon the film thickness are the entrainment speed and the lubricant's viscosity. On the opposite side is the load which has the weakest effect. This is due to the increase of lubricant's viscosity with pressure and the fact that once inside the contact the lubricant cannot escape easily making the lubricant film stiffer than the solid, surrounding surfaces. Equation (1) was validated by experimental results as shown in many publications [11-13].

It can be said that the formation of elastohydrodynamic films and the lubricant film thickness are well understood in steady-state conditions, when the velocity, load and geometry remain unchanged with time. In real-life applications however, steady state is rarely obtained in machine components working in EHD regime of lubrication. For some of these

machine components, like gears and cams the causes of non-steady conditions are first of all intrinsic and result from their geometry and kinematics, which imply large variations of sliding/rolling velocities and of the load. In others, like rolling element bearings steady-state conditions can be achieved when they run at constant speed and under constant load, however transient speed conditions always occur at start and stop of the motion while transient loading is the result of vibrations which are almost inevitably transmitted through the bearing.

Research into the behaviour of elastohydrodynamic films in transient conditions has received merited attention during the relatively recent past, with the focus mainly on geometry and speed variation. The research onto the transient effect of geometry upon the behaviour of EHD films has been driven by studies on mixed lubrication, where roughness plays an important role [e.g. 14-16] and those on surface featured lubrication seen as a way to improve load carrying capacity and reduce friction drag [17-19].

A good deal of papers on transient effects in EHD lubrication considered the behaviour of the lubricant film under rapid variation of velocity of surfaces, in both experimental and numerical approaches. These studies have shown that the transit of the lubricant through the contact, under variable entrainment speed causes fluctuations of the film thickness as any perturbation generated in the inlet travels at the average speed of the surfaces [20, 21]. Under sudden halting of motion, the rapid film decrease is delayed by a squeeze effect eventually leading to fluid entrapments formed inside the contact [22, 23]. Conversely, when the surfaces are suddenly set in motion, oscillations with decreasing amplitude are generated in the film thickness due to the instability created in the inlet of the contact [24, 25]. Similar fluctuations of the film thickness were observed during a step load of the contact [26-28]. This prompts to the conclusion that the elastohydrodynamic film and the surrounding, solid bodies form a mass, spring damper form a dynamic system which responds to a sudden shift from equilibrium in a manner known from vibrations theory [29].

Apart from the sudden application of load, studies concerning the effect of load variation upon the behaviour of EHD films are rare, due probably to the fact that the load has small influence upon the steady-state film thickness and the relatively difficult experimental conditions. Kilali et al. [30] used an optical-based experimental rig combined with a system which superimposed a normal load excitation on the static one to measure the fluid film thickness and the dynamic response of the contact subjected to a harmonic loading. Limited results are presented and none on the response of the film under harmonic vibrations. Sakamoto et al. [31] also applied the optical interferometry technique to directly observe the effects of cyclic pulsating and impact load on EHD point contact under static and rolling/sliding conditions. They observed an oil entrapment formed during rapid increase of the load. The thickness of this entrapment is diminished as the overall entrainment speed of the contact increases.

Morales-Espejel [32], Felix-Quinonez and Morales-Espejel [33] proposed an improved semi-analytical method for evaluating the film thickness fluctuations in the normal-approach of EHD contacts. The method was based on squeeze film effects as well as the variation of lubricant entrainment speed caused by the oscillating load and change of the conditions in the inlet region of the EHD contact. Film thickness results predicted by their semi–analytical method was compared with full numerical simulations. It was concluded that film thickness perturbations could be ascribed to two effects: squeeze film phenomenon caused by vertical rigid body motion of the surfaces and variation in effective entrainment velocity due to fluctuations of contact width.

In the present research the authors conducted experiments on the measurement of the elastohydrodynamic film thickness in contacts subjected to harmonic variation of load. The behaviour of the EHD film was evaluated and, on that basis, a qualitative theoretical analysis was devised and carried out.

3. Experimental setup and working conditions

The EHD film thickness was measured by the optical interferometry technique, described in detail by these and other authors in various publications [34-36]. The schematic of the experimental arrangement is shown in Figure 2. An EHD contact was formed between the flat surface of a glass disc and a highly-polished steel ball. The disc is driven at desired speed by a shaft coupled to an electric motor. The ball is half-immersed in the lubricating fluid and driven by the shear forces developed in the EHD film, resulting in a nominally pure rolling contact. The ball is supported by a shaft which in turn is fitted to a carriage providing bearings support. The ball carriage is attached to a steel bellow, which ensures that vertical displacement can be applied to the ball and that the lubricant does not leak from the lubricant chamber, and a plunger which allows the load to be transmitted to the ball.

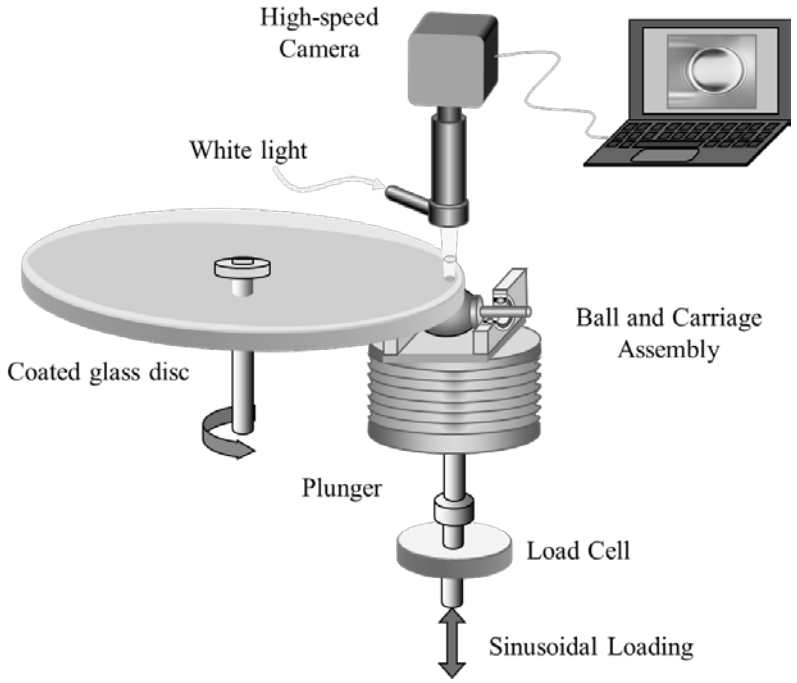

Figure 2. Schematic of the experimental setup

In between a lever which oscillates under the action of a dynamic shaker and the plunger attached to the bellow there was placed a load cell such that the force applied directly to the contact was known. A waveform generator was used to provide a true sinusoidal signal for the shaker. The electrical signal from the load cell was amplified and sent to a digital oscilloscope for visualisation and recording. The dynamic response of the test rig is important in such experiments where some of the parts are subjected to oscillatory motion. For this reason, the rig was designed to be as stiff as possible, given the space limitations. The shaft supporting the ball was made with a relatively large diameter while the bearings supporting this shaft were placed very close to the ball. Moreover, needle bearings were chosen to support the shaft as their linear contacts make them considerably stiffer than ball bearings. In order to minimise the deflection of the glass disc, this was made relatively thick (12 mm) and was also supported by an additional, rolling support diametrally opposite to the location of the studied contact; this prevented the deflection of the disc' shaft. Exact modelling of the dynamic response was not one of the objectives of the paper, however a simplified analysis was carried out, which showed that the natural frequency of the test rig is over 2100 Hz, thus well beyond the maximum frequency employed in these experiments, that is 100 Hz.

The contact was illuminated through the transparent glass disc, which was coated with a thin, semi-reflective chromium layer (5-10 nanometres) and an aluminium oxide layer (approximately 150 nanometres) on the contacting surface. The former was to provide amplitude division of the light waves of a white source while the latter was to increase the gap between the two reflective surfaces that is, chromium and steel. The light rays reflected by these surfaces recombine and interfere constructively or destructively depending of their particular wavelengths resulting in a coloured image of the EHD contact, as seen in Figure 1. These images were captured by a high-speed CCD camera and sent to a laptop computer for storage and analysis. A simple electrical circuit ensured that the camera and oscilloscope recordings were synchronised such that it was precisely known the value of the force loading the contact at each frame time of the camera. Details of this arrangement are provided in [37].

The research encompassed a larger number of lubricants, but the results shown in this paper are for a poly-alpha-olefin synthetic lubricant, PAO40, with kinematic viscosity of 339.8 mm^2/s (339.8 cSt) at 40^oC and 35.8 mm^2/s (35.8 cSt) at 100^oC. The density at 40^oC is 840 kg/m^3. Because PAO40 is a viscous lubricant, it forms a thick film even at low entrainment speeds, thus the results analysed in this paper were obtained at the lowest entrainment speed of the tests of 50 mm/s and ambient temperature of 21±1^oC.

The load applied was varied harmonically between about 1-4 N minimum and 43 N to 56 N maximum, at frequencies of 10 Hz, 25 Hz, 50 Hz, and 100 Hz. This gives a Hertzian pressure variation, for steel on glass, of between approximately 0.2 GPa and 0.7 GPa (the steel ball is 19.05 mm diameter super-finished at 10-15 nanometres Ra). Thousands of cycles of load variation were recorded for each test, showing excellent consistency of the load amplitude in each of these tests. There were variations of the amplitude between tests especially at the largest frequency of 100 Hz. The shaker oscillates in an alternating cycle, while the load variation required was pulsating. In order to deal with this, a constant load was initially applied and with the shaker in operation, this load was adjusted to give the desired load variation to the contact. This was a delicate operation thus it was not always possible to adjust the load exactly between zero and the maximum value. Complications also resulted from the fact that the amplitude of the oscillations of the shaker decreased with the increase of the frequency. The large number of repetitions of each test condition and number of cycles recorded allowed enough good data to be saved for analysis. Table 1 summarises all the operating conditions for different conducted experiments.

Table 1. Test conditions of experiments

Test Lubricant	Kinematic Viscosity	Temperature	Entrainment speed	Frequency	Load Amplitude
PAO 40	339.8 mm^2/s (339.8 cSt) at 40 ^oC 35.8 mm^2/s (35.8 cSt) at 100 ^oC	Ambient 21±1^oC	0.05 m/s	10 Hz	1-52 N
				25 Hz	0.7-53 N
				50 Hz	0.6-56 N
				100 Hz	2-43 N

4. Experimental results

Figures 3 to 6 show the load variation, at four different frequencies and a number of seven interferometry images of the contact selected to cover one cycle of load variation. The black dots on each of the load-variation cycles correspond to the time location of the selected images within the cycle. The time-stamp for each image as well as the direction of the entrainment motion are shown on the images. As seen the load varies on a fashion that approximates well a sinusoid curve.

It is well-known that in white light interferometry various colours signify variation of the gap between the surfaces, thus different film thicknesses of the lubricant film. It is thus immediately noticed from the images shown that, for all frequencies, the film thickness is different in the load-increasing and load-decreasing phases. It is also obvious from these images that the EHD film behaves differently depending on the frequency of the load variation. For the lowest frequency, that is 10 Hz the typical EHD film image is shown with a large, central area of nearly constant thickness, however, at the largest two frequencies, 50 Hz and 100 Hz rings of different colours are seen inside the contact, indicating relatively large variation of the film thickness within the contact area. The reasons for this behaviour will be discussed in the following section.

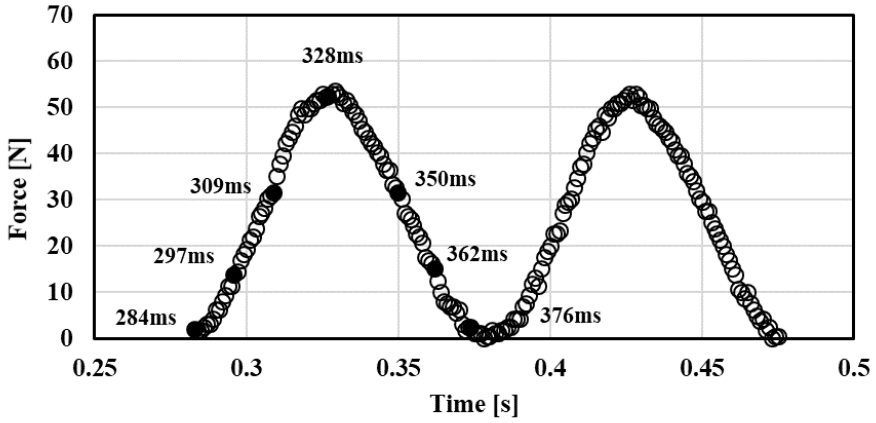

Figure 3a. Example of load variation, 10 Hz, PAO 40

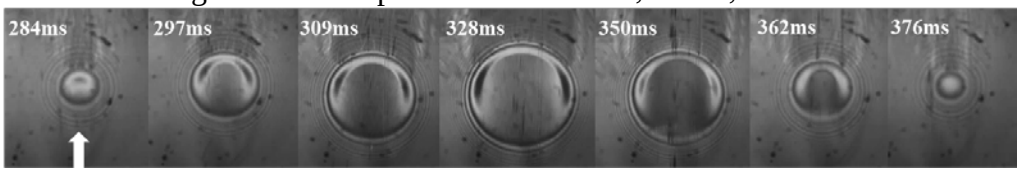

Figure 3b. Interferograms of the PAO 40 at ambient temperature, captured at 10 Hz

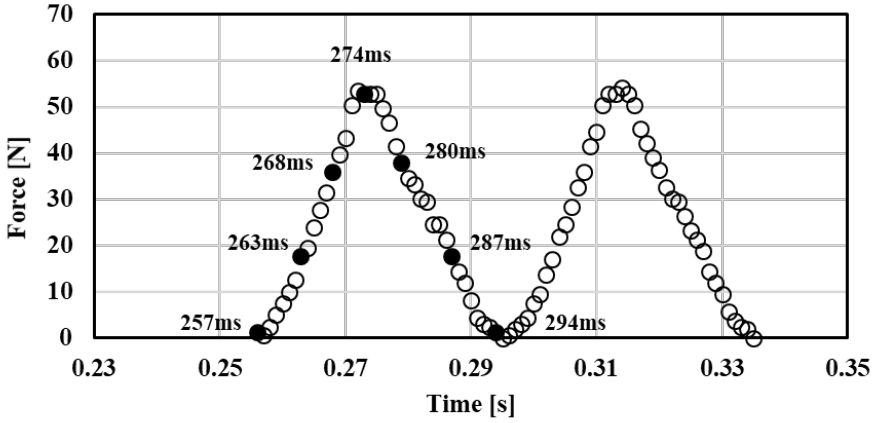

Figure 4a. Example of load variation, 25 Hz, PAO 40

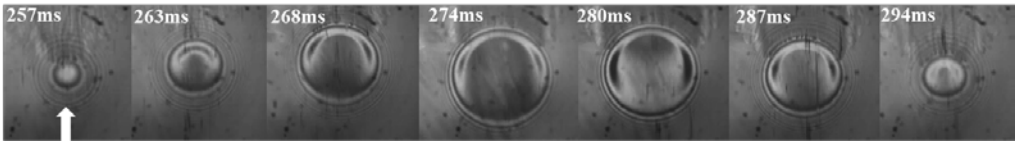

Figure 4b. Interferograms of the PAO 40 at ambient temperature, captured at 25 Hz

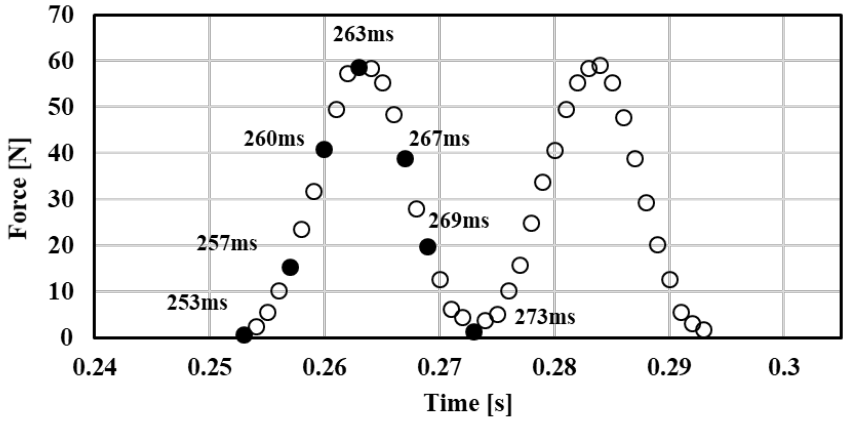

Figure 5a. Example of load variation, 50 Hz, PAO 40

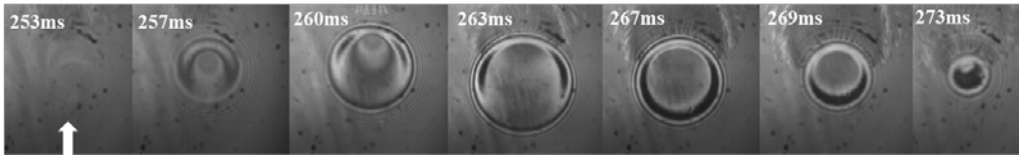

Figure 5b. Interferograms of the PAO 40 at ambient temperature, captured at 50 Hz

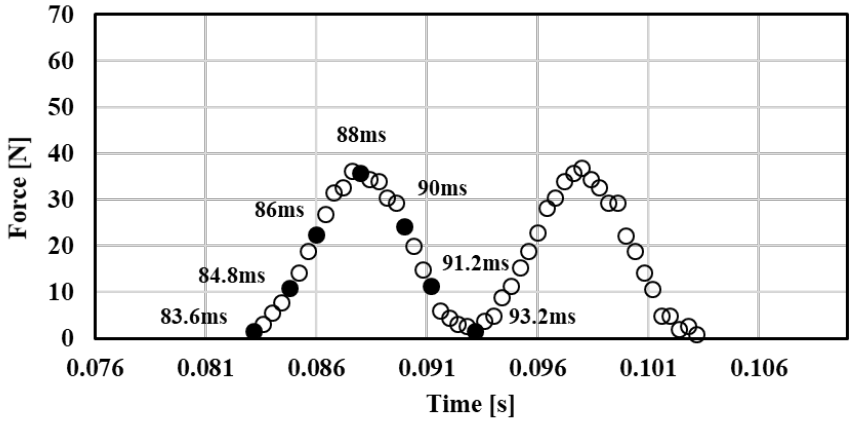

Figure 6a. Example of load variation, 100 Hz, PAO 40

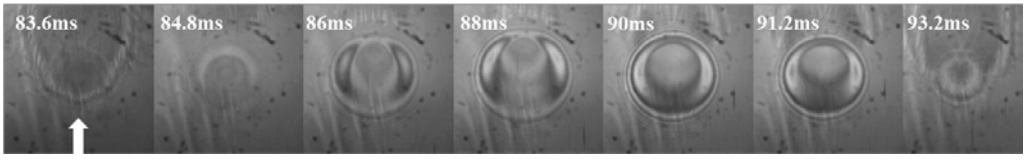

Figure 6b. Interferograms of the PAO 40 at ambient temperature, captured at 100 Hz

5. Discussion

5.1. Experimental observations

The interferometry images shown in figures above were converted into film thickness maps according to a calibrations procedure which relates the RGB colour content in every pixel of the image to a lubricant film thickness value. Details of the calibration procedure and an accuracy analysis are presented in [37]. Figure 7 shows the variation of the load, and central film thickness over one cycle, for the four frequencies employed in these experiments. In all these the entrainment speed set was 0.05 m/s.

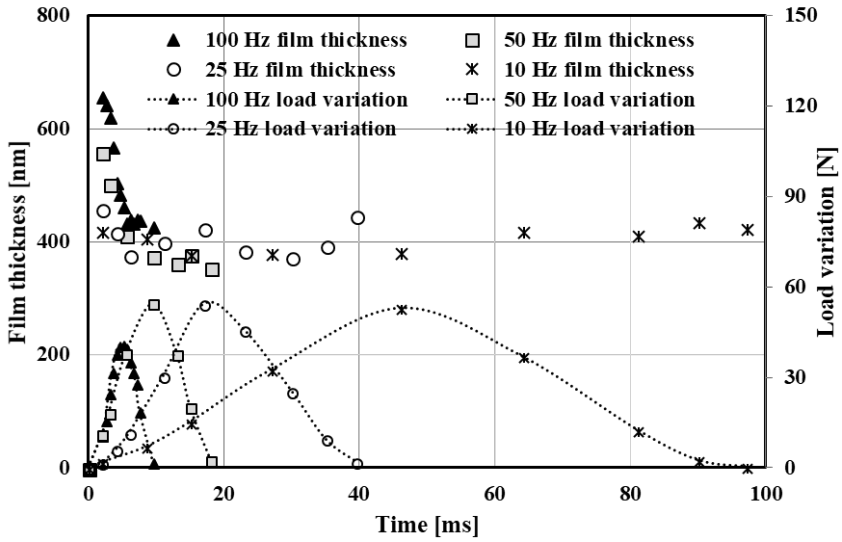

Figure 7. Central film thickness at four frequencies, 0.05 m/s

Given the fact that the load variation is approximately symmetric in the increasing and decreasing phases, it would be expected that the film thickness variation is also symmetric, which, as seen it is not the case. For the larger frequencies the central film thickness is much larger during the load-increasing than in the load-decreasing phase. This is better observed in Figure 8 which shows the relative variation over one cycle. The theoretical film thickness, calculated from the measured load and entrainment speed is also shown. T is the period of the given cycle of load variation. As seen there is a strong difference of the behaviour of the elastohydrodynamic film depending of the frequency of the load variation.

The theoretical film thickness (Eq. 1) varies little with load, as expected, even if this parameter changes more than 15 times, however the experimental values show large variation over the load cycle at the largest frequency of 100 Hz.

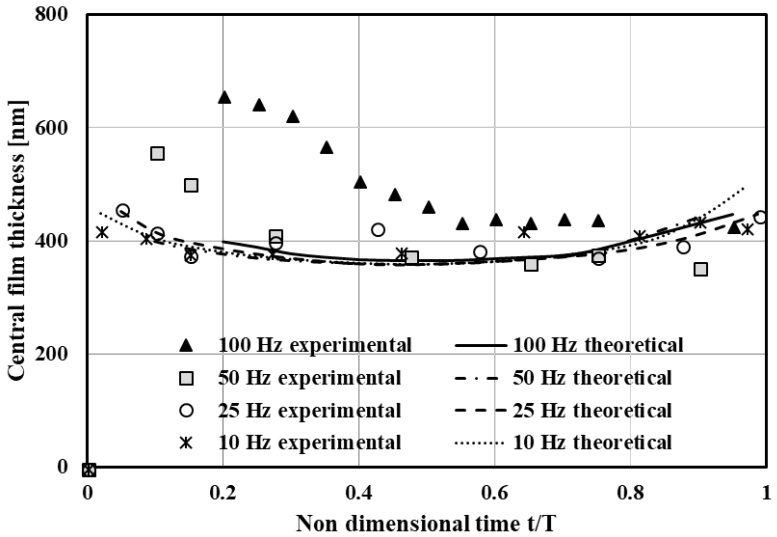

Figure 8. Central film thickness variation over one cycle

At the beginning of the load-increasing phase the measured film thickness is about 65 percent larger than the theoretical, steady-state value. It drops continuously towards the later

and becomes smaller (about 95 percent) when the load approaches the minimum value in the load-decreasing phase. At 50 Hz, the transient experimental film thickness is just under 40 percent larger than the steady-state value, at the beginning of the load increasing phase and about 20 percent lower when the load reaches the lowest value of the cycle. At the two lowest frequencies 10 Hz and 25 Hz, the experimental values follow the theoretical one, within the error of the method, over the whole cycle.

5.2. Analytical modelling

The EHD film thickness is established by the conditions in the inlet of the contact, as mentioned above. In the current experiments the entrainment velocity was kept constant at 50 mm/s. It is now assumed that the load varies between zero and a given value $2P_o$ on a sinusoidal fashion, as expressed by Equation 3.

$$P(t) = P_0(1 + \sin \omega t) \tag{3}$$

It is obvious that, during half a cycle the contact size expands rapidly due to the variation of the load. At the inlet of the contact this expansion is equivalent to an increase of the entrainment velocity during the load-increasing phase and a decrease during the decreasing of the load. As the contact edge moves in direction opposite to the lubricant entrainment direction, the lubricant approaches the convergent gap at a velocity equal to the sum of the velocity of the contact edge and the mean velocity of the surfaces. It results and a net (effective) entrainment velocity larger than that corresponding to steady state conditions. According to Hertz's theory of elastic bodies contact the radius of contact between a sphere and a plane depends of the load, the radius of the sphere and the elastic modulus of the contacting bodies [38]. In order to evaluate the transient entrainment speed, the radius of the contact is written as a function of time as shown in Equation 4.

$$a = \left(\frac{3R}{4E^*}\right)^{1/3} P(t)^{1/3} \tag{4}$$

The speed of change of the contact radius is da/dt, so combining (3) and (4) we get:

$$\frac{da}{dt} = \frac{da}{dP}\frac{dP}{dt} = \frac{1}{3}\left(\frac{3R}{4E^*}\right)^{1/3} P(t)^{-2/3} P_0 \omega \cos \omega t = \left(\frac{RP_0}{36E^*}\right)^{1/3} \frac{\omega \cos \omega t}{(1+\sin \omega t)^{2/3}} \tag{5}$$

This relationship shows that the speed is different in the load increasing and load decreasing phases, as the functions sine and cosine are out of phase by T/4. Another observation is that the speed becomes infinite when sinus equals -1 that is when the load is zero. Obviously that in reality the film thickness cannot be zero, and to avoid this, the entrainment velocity was set to zero when the load was zero. This is illustrated in Figure 9 which shows the velocity of the contact radius change, the set, rolling speed and the resultant or effective entrainment velocity. The load amplitude was taken as 20.5 N to match the experimental values for the 100 Hz tests.

It can be seen that, as a result of the harmonic load variation, the effective entrainment velocity is larger than the rolling speed of the surfaces during the load increasing-load phase and smaller during the load decreasing phase. At its peak the effective entrainment speed is over 3 times the rolling speed, which obviously would affect the EHD film thickness. In order to evaluate the transient film thickness, the formula given by Equation (1) is written as:

$$h_c = A \cdot u^{2/3} P(t)^{-2/30} \tag{6}$$

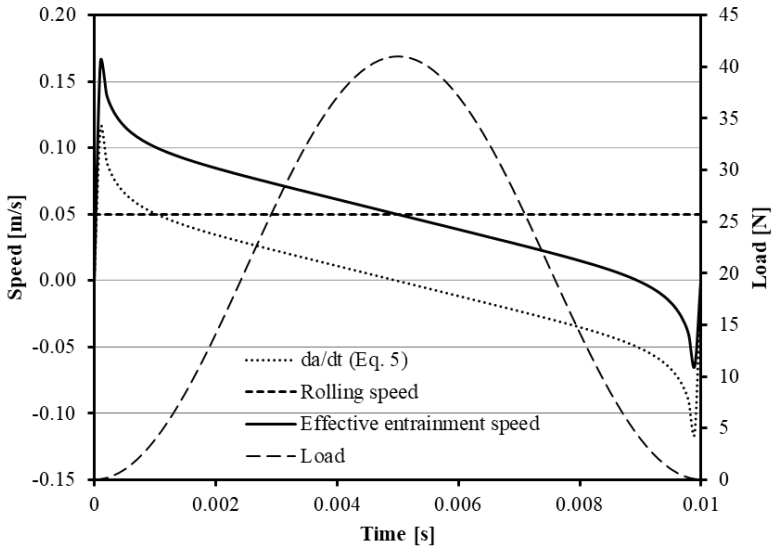

Figure 9. Entrainment velocity in transient load conditions

In equation (1), 0.67 was approximated by 2/3 and 0.067 by 2/30, while A is a constant factor which include all parameter except velocity and load. According to the above analysis the effective entrainment velocity is equal to the rolling velocity and the velocity of change of the contact radius; the transient film thickness can thus be written as:

$$h(t) = A \cdot \left(u_0 + \frac{da}{dt} \right)^{2/3} P(t)^{-2/30}, \tag{7}$$

where u_o is the constant rolling speed. If u_o is brought in front of the bracket and taking into account equation (5) the time-dependent film thickness becomes:

$$h(t) = A \cdot u_0^{2/3} \left[1 + \frac{1}{u_0} \left(\frac{RP_0}{36E^*} \right)^{1/3} \frac{\omega \cos \omega t}{(1+\sin \omega t)^{2/3}} \right]^{2/3} P(t)^{-2/30} \tag{8}$$

Using (6) the ratio of transient to steady-state film thickness (EHD film thickness calculated with formula (1) but with the load varying by (3) at each time step) can be written as:

$$\frac{h(t)}{h_{st}} = \left[1 + \frac{1}{u_0} \left(\frac{RP_0}{36E^*} \right)^{1/3} \frac{\omega \cos \omega t}{(1+\sin \omega t)^{2/3}} \right]^{2/3} \tag{9}$$

The variation of this ratio, together with the normalized load (current load/ maximum load) as a function of non – dimensional time (time/period of load cycle) is shown in Figure 10. The parameters of this simulation are: frequency 100 Hz, load variation amplitude 20.5 N, entrainment speed 0.05 m/s. This graph shows that at the beginning of the load–increasing phase the transient film thickness is more than two times larger than the theoretical film thickness. As the load increases towards its maximum value, the transient film thickness tends towards the steady state value.

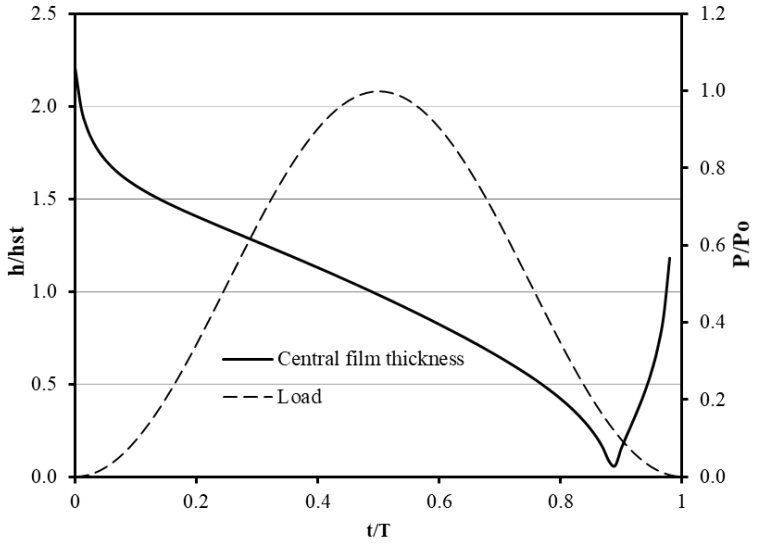

Figure 10. Ratio of transient film thickness and steady state film thickness at 100 Hz

It can be seen that, at a certain moment during the cycle the film thickness becomes zero due to the fact that the effective entrainment velocity momentarily becomes zero as seen in Figure 9. A pertinent question can be asked for the variation of the film thickness over the whole cycle: why are the values of the film thickness at the beginning and the end of the cycle not equal? The answer is that they are, but because they are infinite they cannot be shown in the graph. At the beginning of the cycle, the load is zero and obviously in this case Hamrock and Dowson equation (1) predicts infinite film, or rather no film.

5.3. The effect of working parameters

The effect of the working parameters can be evaluated from relationship (9). The larger the frequency the quicker the load increases and consequently the effective entrainment speed. Figure 11 shows the central film thickness for four frequencies at constant load amplitude of 20.5N and a set entrainment speed of 0.05 m/s.

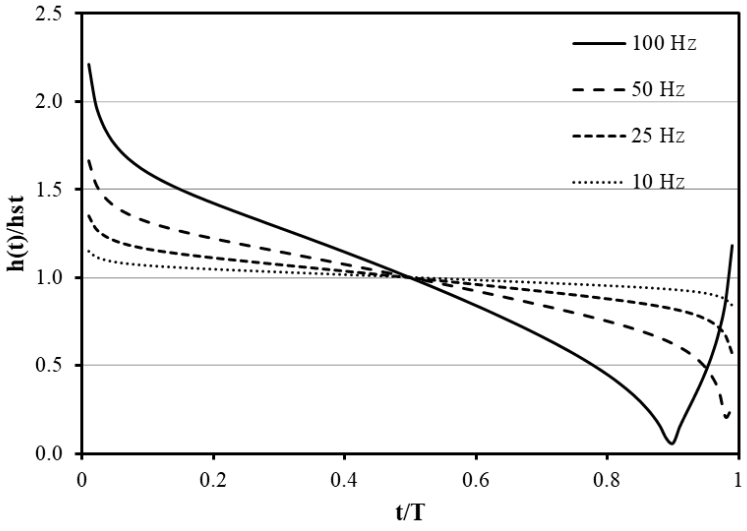

Figure 11. The effect of frequency upon central film thickness

It can be seen that at lower frequencies the film thickness is almost equal to the steady state value over the whole vibration cycle, while at the largest frequency employed in these tests, 100 Hz, the transient formula predicts a film thickness 2.3 times larger than steady state at the beginning of the vibration cycle.

Figure 12 shows the variation of the maximum film thickness with the frequency of load variation.

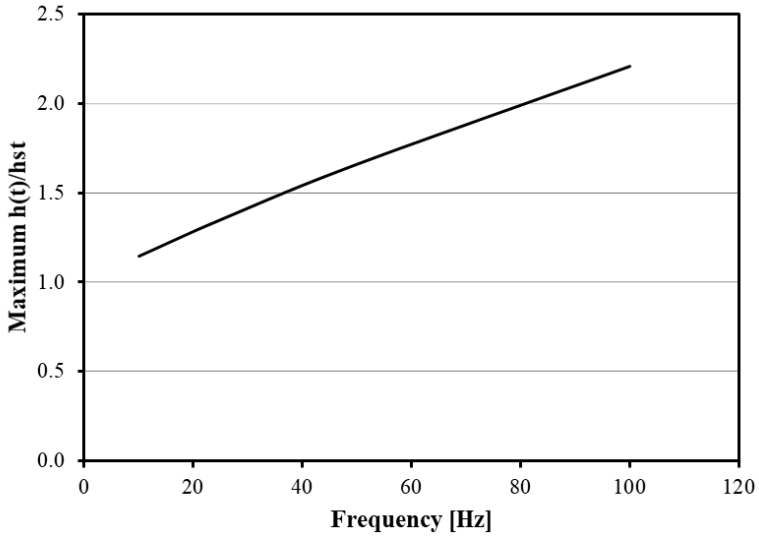

Figure 12. The variation of maximum transient film thickness with frequency

Hooke and Morales-Espejel [39] performed a theoretical analysis of line contacts subjected to load fluctuations, on a non-zero mean cycle. The conditions of the current experiments are obviously quite different from those in [39] however it is interesting to make a similar evaluation of the effect of frequency upon maximum film thickness variation. The same non-dimensional parameters for wavelength, $\lambda/b\ P^{1.5}S^{-2}$ and maximum film thickness variation, $\delta hE'/\delta F\ P^{0.75}S^{-1}$, with $\lambda = u/f$, $P = \alpha P_H$, *and* $S = GU^{0.25}$. In these u is the mean surfaces velocity, f is the frequency, α the pressure-viscosity coefficient, P_H the Hertzian pressure, $G = \alpha E'$ the material parameter and $U = (\eta_0 u/E'R)$. The conditions used in current tests give the Greenwood pressure parameter P of 14.2 and Greenwood speed parameter S = 6.8 and an inlet piezoviscous parameter $c = 0.967P^{0.2}S^{0.8}$ of 7.6. In [39] film thickness variation is given for values of P = 20 and S = 8, while c ranged between 2 and 20. The non-dimensional film thickness versus non-dimensional wavelength, for the four frequencies employed in these tests is shown in figure 13. The trend of this variation is very similar to that seen in figure 3a of reference [39], even accounting for the differences in the conditions used. It is obvious that the frequencies employed in the current tests are small enough such that the maxima of film thickness seen in [39] it is not reached.

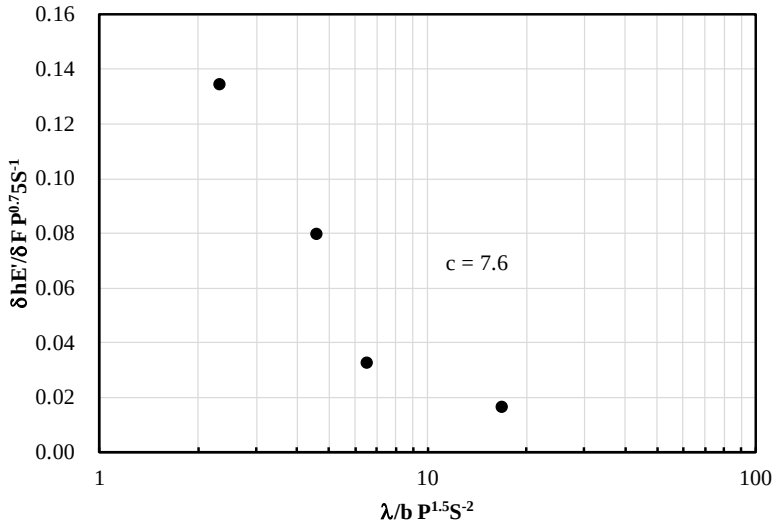

Figure 13. Non-dimensional film thickness variation with non-dimensional wavelength

Another parameter which strongly influences the transient behaviour of EHD films is the entrainment speed of the contact. This effect is shown in figure 14 where the frequency was kept constant at 100 Hz and the entrainment speed (constant, set rolling speed, independent of the load variation) changes as seen. Is it obvious that an increase of entrainment speed is equivalent to a decrease of the frequency.

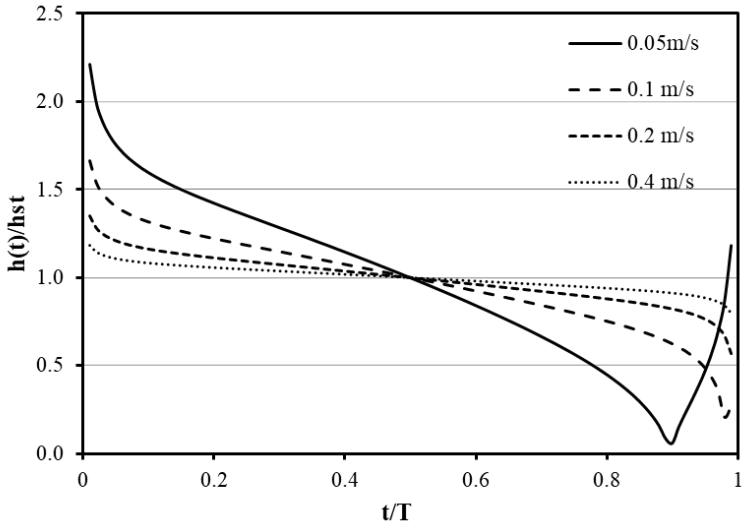

Figure 14. The effect of entrainment speed upon transient film thickness

Finally, the other parameter which influences the film thickness, in transient conditions, is the load amplitude. Figure 15 shows this effect for a contact running at the same frequency of 100 Hz and an entrainment speed set at 0.05 m/s.

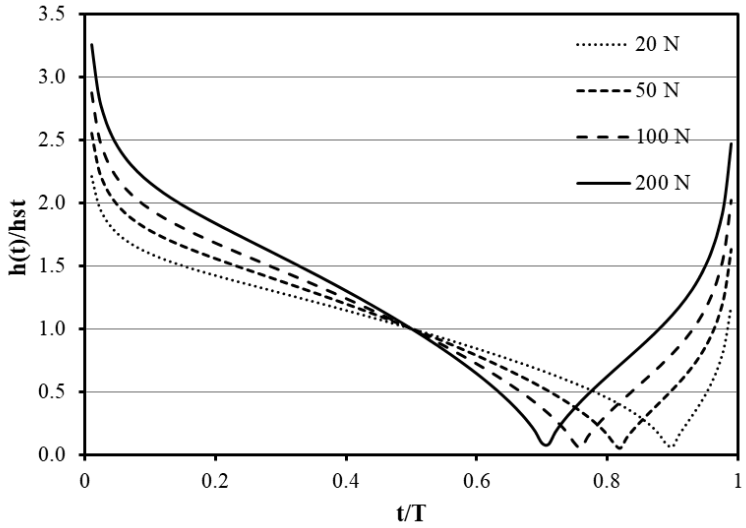

Figure 15. Effect of load amplitude upon transient film thickness

It is known that the effect of the load upon the steady state film thickness is almost negligible, in comparison to the effect of speed for example, however as seen in figure 15 in case of transient films this parameter influences the film thickness as strongly as the entrainment speed. This is because by keeping the frequency constant, the change of the amplitude of the load is equivalent to a more rapid variation of contact dimensions, thus the entrainment speed increases, according to equation (7).

5.4. Comparison of experiment and theory

This theoretical analysis was intended to give a qualitative and not quantitative insight to the behaviour of film thickness under cyclically load variation, however it is interesting to make a direct comparison to experimental values of the film thickness. Figure 16 shows such comparison. Obviously, the experimental values show a descending trend, like the theoretical curve, and reasonably agree with the later for a part of the cycle. It is clear that at the beginning and end of the load variation cycle, where the effective entrainment velocity is largest and thus the squeeze effect is expected to be strongest, the measured values differ from the theoretical ones. The difference is especially great during the second half of the cycle, where the rapid decrease of the load makes the effective entrainment velocity drop rapidly and change sign, thus making the theoretical film thickness momentarily zero. At this moment the film thickness in the central region of the contact does not follow the speed and maintains large values due to the fact that the fluid cannot be squeezed out of the contact quickly enough.

As mentioned previously, squeeze and the time taken for the lubricant to travel across the contact are phenomena not taken into account in this theoretical analysis. The squeeze effect during the rapid decrease of the velocity (and the film thickness with it) results into a film larger than the steady state predictions, by the formation of a lubricant entrapment, as proved experimentally and theoretically [40-43].

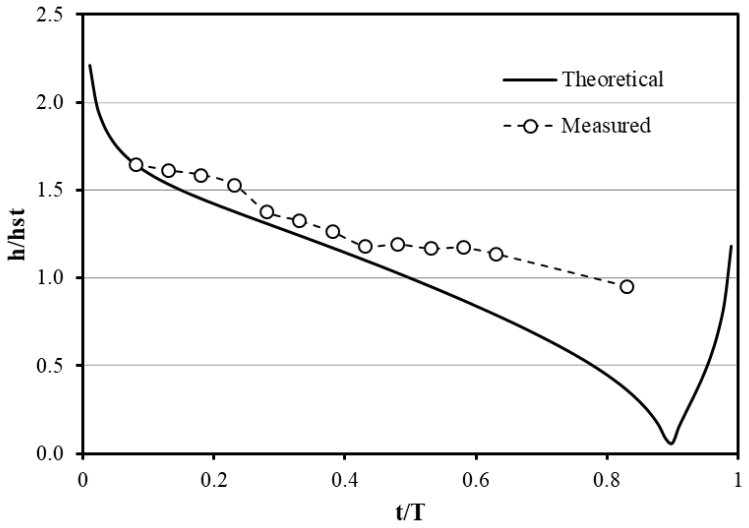

Figure 16. Comparison between theoretical and experimental central film thickness (50 Hz, 20.5 N amplitude, 0.05 m/s)

The current approach and results are supported by the results of the analytical/numerical investigation carried out in [32, 33], which conclude that between the increase of speed due to rapid increase of contact dimensions and the squeeze effects the former is dominant.

This qualitative analysis is evidently simplified and does not take into account the squeeze effect and the time of passage of the lubricant through the contact, however it is able to explain, at least partially the behaviour of the film under cyclically variable loading.

6. Conclusions

Optical interferometry technique was used to measure the film thickness in an elastohydrodynamic contact, formed between a glass disc and a steel ball, subjected to harmonic variation of load. Apart from the ball and disc the system comprised a white light source, a high-speed CCD camera, an electrodynamic shaker and a load cell for measuring the load applied to the contact. Interferometry images of the contact under vibrations were captured, recorded and analysed for film thickness over the contact area.

It was found that the lubricant central film thickness is significantly larger than that corresponding to steady state application of the load during the load increasing phase; about sixty percent larger for the conditions of these tests. During the load decreasing phase the central film thickness drops to values near and slightly below the steady state condition.

A theoretical, analytical modelling of the film thickness behaviour during harmonic variation of load was carried out, based on the theoretical film thickness formula of Hamrock and Dowson. It was shown that the rapid increase of the contact dimensions is equivalent, in the inlet of the contact, with an increase of the effective entrainment speed. Consequently, the film thickness is larger than the steady state predictions during the load increasing phase and smaller during the load decreasing phase. During the load decreasing phase the theoretical, transient film thickness momentarily falls to zero, at large frequencies and rather low set entrainment speed, although the measured results did not show this behaviour. This was explained by the squeeze effect, which prevents the lubricant to escape too quickly from the contact during the rapid decrease of the effective entrainment speed, and the formation of a lubricant entrapment.

Analyses of the effect of frequency, load amplitude and set entrainment speed were carried out, revealing that the frequency and amplitude of the load cycle have an opposite effect to the set entrainment speed.

The current paper provides a simple theoretical tool for prediction of lubricant film thickness in elastohydrodynamic contacts subjected to cyclic or non-cyclic variation of load. Unlike other approaches to this problem, the present analysis does not involve sophisticated numerical analysis tools.

7. References

[1] A. Cameron, 1985, "Righting a 40–year–old wrong", Trib. Int., 18, comment, 92

[2] A. Cameron, "Principles of lubrication", Longmans, 1966

[3] R. Gohar and A. Cameron, 1963, "Optical Measurement of Oil Film Thickness under Elastohydrodynamic Lubrication", Nature, 200, 458-459

[4] R. Gohar and A. Cameron, 1967, "The Mapping of Elastohydrodynamic Contacts", ASLE Trans, 10, 215-225

[5] J. A., Greenwood, 1972, "An extension of the Grubin theory of lubrication", J. Physics. D. Appl. Phys., 5, 2195-221

[6] J.F. Archard, and M. T. Kirk, 1961, "Lubrication of point contacts", Proc. Roy. Soc. Series A, 261, 532 – 550

[7] A. Cameron and R. Gohar, 1966, "Theoretical and experimental studies of the oil film in lubricated point contact", Proc. Roy. Soc., Series A, 291, 520-536

[8] D. Dowson and G. R. Higginson, 1966, "Elastohydodynamic Lubrication, The fundamentals of Roller and Gear Lubrication", Pergamon Press, Great Britain

[9] B. J. Hamrock and D. Dowson, "Isothermal Elastohydrodynamic Lubrication of Point Contact, Part 3-Fully Flooded Results", 1977, Transactions ASME, Journal of Lubrication Technology, 99, 264-276

[10] R. J. Chittenden, D. Dowson, J. E. Dunn and C. M. Taylor, 1985, "A theoretical analysis of the isothermal elastohydrodynamic lubrication of concentrated contacts I: direction of lubricant entrainment coincident with the major axis of the contact ellipse", Proc. R. Soc. London, A397, 345-369

[11] M. Smeeth, and H.A. Spikes, 1997, "Central and Minimum Elastohydrodynamic Film Thickness at High Contact Pressure" J. Trib., 119 (2), 291-296

[12] M. Hartl, I. Krupka, R. Poliscuk, M. Liska, J. Molimard, M. Querry and P. Vergne, 2001, "Thin Film Colorimetric Interferometry", Trib. Transactions, 44:2, 270-276

[13] R. P. Glovnea, A. V. Olver, and H. A. Spikes, 2005, "Experimental investigation of the effect of speed and load on film thickness in EHD contacts" Trib. Trans., 48, 2, 328-335

[14] G. Guanteng, P. M. Cann, H. A. Spikes and A. V. Olver, 1999, "Mapping of Surface Features in the Thin Film Lubrication Regime", Proc. 1998 Leeds Lyon Trib. Symp. Elsevier Tribology Series 36, Ed. D. Dowson, 175-183

[15] M. Kaneta and H. Nishikawa, 1999, "The effects of a Transversely Oriented Bump on Point Contact EHL Films in Reciprocating Motion with a Short Length Stroke", Lubrication at the FrontierD. Dowson et al. Ed., Elsevier B.V., 185-192

[16] J. W. Choo, R. P. Glovnea, A. V. Olver and H. A. Spikes, 2003, "The effect of 3D model surface roughness features on lubricant film thickness in EHL contacts", ASME Trans. J. Trib., 125, 3, 533-542

[17] X. Wang, K. Kato, K. Adachi, and K. Aizawa, 2003, "Load carrying capacity map for the surface texture design of SiC thrust bearing sliding in water", Trib. Int., 36, 189-197

[18] L. Mourier, D. Mazuyer, A. A. Lubrecht and C. Donnet, 2006, "Transient increase of film thickness in micro-textured EHL contacts", Trib. Int. 39, 1745-1756

[19] I. Krupka and M. Hartl, 2006, "The effect of surface texturing on thin EHD lubrication films", Trib. Int., 40, 1100-1110

[20] C. J. Hooke, 1993, “The minimum film thickness in line contacts during reversal of entrainment,” Trans. ASME, J. of Tribology, Vol. 115, 191-199
[21] J. Sugimura, W.R. Jr Jones and H. A. Spikes, 1998, “EHD film thickness in non-steady state contacts,” Trans. ASME, J. of Tribology, Vol. 120, 442-452
[22] R. P. Glovnea and H. A. Spikes, 2000, “The influence of lubricant on film collapse rate in high pressure thin film behaviour during sudden halting of motion,” STLE Trib. Trans., 43, 4, 731-739
[23] M. J. A. Holmes, H. P. Evans and R. W. Snidle, 2003, “Comparison of Transient EHL Calculations with Shut-down Experiments”, Tribology and Interface Engineering Series, Vol. 41, 79-89
[24] R. P. Glovnea and H. A. Spikes, 2001, “Elastohydrodynamic film formation at the start-up of the motion” Proc. I. Mech. Eng., Vol. 215, J. Eng. Trib., 125-138
[25] G. Popovici, G. H. Venner and P. M. Lugt, 2004, “Effects of Load System Dynamics on the Film Thickness in EHL Contacts During Start-up”, ASME Trans., J. Trib., 126, 258-266
[26] R. Larsson and J. Lundberg, 1998, “Observations in transiently loaded EHL contacts under pure sliding conditions”, STLE Trib. Trans., 41, 4, 489-496
[27] Y. H. Wijnant, C. H. Venner, R. Larsson and P. Eriksson, 1999, “Effects of Structural Vibrations on the Film Thickness in an EHL Circular Contact”, J. Trib. 121, 259-264
[28] M. Kaneta, S. Ozaki, H. Nishikawa and F. Guo, 2007, “Effects of impact loads on point contact elastohydrodynamic lubrication films”, Proc. I.Mech.E., J. Eng. Trib., 221, 271-278
[29] S. S. Rao, “Mechanical Vibrations”, Pearson, 2016
[30] T. El Kilali, J. Perret-Liaudet and D. Mazuyer, 2004 “Experimental analysis of a high pressure lubricated contact under dynamic normal excitation force”, Transient Processes in Tribology, 43, 409-418
[31] M. Sakamoto, H. Nishikawa and M. Kaneta, 2004, “Behavikaor of Point Contact EHL Films Under Pulsating Loads”, Trans. Proc. Trib., Elsevier, 391-399
[32] G. EMorales-Espejel, 2008, Central film thickness in time-varying normal approach of rolling elastohydrodynamically lubricated contacts, Proc. IMechE Vol. 222, Part C: J. Mech. Eng. Sci.
[33] A. Felix-Quinonez and G. E. Morales-Espejel, 2010, “Film thickness fluctuations in time-varing normal loading of rolling elastohydrodynamically lubricated contacts”, Proc. IMechE, 224, Part C: J Mech. Eng. Sci.
[34] G. J. Johnston, R. Wayte and H. A. Spikes, 1991, “The Measurement and Study of Very Thin Lubricant Films in Concentrated Contacts”, Tribology Transactions, 34, 2, 187-194
[35] P. M. Cann, H. A. Spikes and J. Hutchinson, 1996, “The development of a Spacer Layer Imaging Method (SLIM) for Mapping Elastohydrodynamic Contacts”, Tribology Transactions, 39, 4, 915-921
[36] O. Marklund and L. Gustafsson, 2001, “Interferometry-based Measurements of oil-film thickness”, Proc Instn Mech Engrs, 215, Part J, 243-259
[37] X. Zhang, 2017, “The effect of vibrations on the behaviour of elastohydrodynamic contacts”, PhD thesis, University of Sussex
[38] K. L. Johnson, 1985, “Contact Mechanics”, Cambridge University Press, United Kingdom
[39] C.J. Hooke and G. E. Morales-Espejel, 2016, “The effect of small sinusoidal load variations in elastohydrodynamic line contacts”, ASME, J. Trib., 138, 031501-9
[40] P. R. Yang and S. Z. Wen, 1991, “Pure squeeze action in an isothermal elastohydrodynamic lubricated spherical conjunction, Part 1: Theory and dynamic load results”, Wear, 142, 1-16

[41] Glovnea, R.P. and Spikes, H.A., “Elastohydrodynamic Film Collapse During Rapid Deceleration – Part I: Experimental Results,” ASME Trans. Journal of Tribology, 123, 2, (2001), 254-261

[42] Glovnea, R.P. and Spikes, H.A., “Elastohydrodynamic Film Collapse During Rapid Deceleration – Part II: Theoretical Analysis and Comparison of Theory to Experiment,” ASME Trans. Journal of Tribology, 123, 2, (2001), 262-267

[43] F. Guo, H. Nushikawa, P. Yang and M. Kaneta, 2007, “EHL under cyclic squeeze motion”, Trib. Int. 40, 1–9